NASA TECHNICAL MEMORANDUM

NASA TM X-2646

NASA TM X-2646

COMPARISON OF NEUTRON SPECTRA MEASURED WITH THREE SIZES OF ORGANIC LIQUID SCINTILLATORS USING DIFFERENTIATION ANALYSIS

by Donald F. Shook and Clarence R. Pierce

Lewis Research Center

Cleveland, Ohio 44135

NATIONAL AERONAUTICS AND SPACE ADMINISTRATION • WASHINGTON, D. C. • NOVEMBER 1972

1. Report No.	2. Government Accession No.	3. Recipient's Catalog No.
NASA TM X-2646		

4. Title and Subtitle	5. Report Date
COMPARISON OF NEUTRON SPECTRA MEASURED WITH THREE SIZES OF ORGANIC LIQUID SCINTILLATORS USING DIFFERENTIATION ANALYSIS	November 1972
	6. Performing Organization Code

7. Author(s)	8. Performing Organization Report No.
Donald F. Shook and Clarence R. Pierce	E-6883
	10. Work Unit No. 503-10

9. Performing Organization Name and Address	11. Contract or Grant No.
Lewis Research Center National Aeronautics and Space Administration Cleveland, Ohio 44135	
	13. Type of Report and Period Covered
12. Sponsoring Agency Name and Address	Technical Memorandum
National Aeronautics and Space Administration Washington, D. C. 20546	14. Sponsoring Agency Code

15. Supplementary Notes

16. Abstract

Proton recoil distributions were obtained by using three organic liquid scintillators of different size. The measured distributions are converted to neutron spectra by differentiation analysis for comparison to the unfolded spectra of the largest scintillator. The approximations involved in the differentiation analysis are indicated to have small effects on the precision of neutron spectra measured with the smaller scintillators but introduce significant error for the largest scintillator. In the case of the smallest cylindrical scintillator, nominally 1.2 by 1.3 cm, the efficiency is shown to be insensitive to multiple scattering and to the angular distribution of the incident flux. These characteristics of the smaller scintillator make possible its use to measure scalar flux spectra within media where high efficiency is not required.

17. Key Words (Suggested by Author(s))	18. Distribution Statement
Neutron spectra; Organic scintillator; Neutron flux measurement; Spectra unfolding; In-core spectrum measurement	Unclassified - unlimited

19. Security Classif. (of this report)	20. Security Classif. (of this page)	21. No. of Pages	22. Price*
Unclassified	Unclassified	28	$3.00

* For sale by the National Technical Information Service, Springfield, Virginia 22151

COMPARISON OF NEUTRON SPECTRA MEASURED WITH THREE SIZES OF ORGANIC LIQUID SCINTILLATORS USING DIFFERENTIATION ANALYSIS

by Donald F. Shook and Clarence R. Pierce

Lewis Research Center

SUMMARY

Proton recoil pulse height distributions obtained by using three organic liquid scintillators of different size are converted to neutron spectra by differentiation analysis. The approximations involved in this analysis are indicated to have small effects on the precision of neutron spectra measured with the smaller scintillators but introduce significant error for the largest scintillator. The data were obtained by using three cylindrical scintillators nominally 1.2 by 1.3, 2.2 by 2.4, and 5.0 by 5.0 centimeters.

For the largest scintillator, an unfolding analysis employing calibrated monoenergetic response functions was used as a reference. All four measurements agree on the measured shape of a polonium-beryllium neutron source spectrum, but absolute fluxes obtained with the largest scintillator by differentiation analysis are 10 to 20 percent lower than the fluxes obtained by using the calibrated unfolding analysis. However, absolute fluxes obtained with the two smaller scintillators by differentiation analysis agree with fluxes measured by using the calibrated scintillator. This agreement indicates that for small scintillators errors in the analytic expression for efficiency and multiple scattering corrections used in the differentiation analysis are insignificant.

In the case of the smallest scintillator, the efficiency is shown to be insensitive to multiple scattering and to the angular distribution of the incident flux. This characteristic of the smaller scintillator makes possible its use for measuring scalar flux spectra within media where high efficiency is not required. The resolution of the smallest scintillator is indicated to be 50 percent better than that of the largest. The computer code TUNS, which was written to analyze proton recoil pulse height data by the differentiation method, is described.

INTRODUCTION

The method of measuring fast neutron spectra by analysis of proton recoil pulse height distributions obtained with organic scintillators has received considerable attention (refs. 1 and 2). Using organic liquid scintillators and new electronic circuits which permit separation of gamma ray signals allows a differential proton recoil spectrum to be obtained which shows significant spectral detail. A number of methods are available for converting the measured proton recoil spectrum into the incident neutron energy spectrum, and it is the differentiation method of analysis that is primarily considered in this report. This method was first applied in the early 1960's (ref. 1), but was not widely used because (1) instrumentation in use at that time did not permit measurement of highly accurate proton recoil spectra, (2) the differentiation method involves a calculation of scintillator efficiency with corrections for multiple scattering and wall effects that are difficult to evaluate, (3) the method was not verified by direct comparison with precise calculations or other methods of measurement, and (4) an experimental problem due to the light output anisotropy of stilbene crystals existed.

More recently proton recoil spectra have been measured by using liquid scintillators in conjunction with monoenergetic response functions and the proton recoil data unfolded (ref. 2). The method of differentiation analysis is reexamined in this report in the light of the recent developments because it offers more flexibility than does unfolding analysis.

In this report proton recoil distributions are obtained by using three sizes of organic liquid scintillators. The consistent set of absolute measurements of the same polonium-beryllium (PoBe) neutron source with different sized scintillators was taken to test the differentiation method of data reduction in which the approximations used are expected to be dependent on scintillator size. For reference, a comparison is also made with an unfolding analysis for the measurements made with the 5-centimeter-diameter by 5-centimeter-high scintillator for which calibrated monoenergetic response functions are available (ref. 2). The unfolding analysis is not subject to uncertainties due to multiple scattering and wall effect corrections since a large set of measured monoenergetic response functions for the specific scintillator are used. If the spectrometer is employed in exactly the same geometry as the response functions have been measured, the unfolded spectra should be accurate, although the error in the unfolded spectra due to the error in the response functions is difficult to evaluate. The accuracy of the unfolding method has been tested by comparing neutron spectra by both the unfolding and time-of-height techniques with reasonable success (ref. 3). The characteristics of the smallest scintillator used are emphasized in this report. In particular, the improved resolution and applications of this scintillator, as summarized in reference 4, are discussed.

EXPERIMENT

The measurements were made by using a PoBe neutron source circulated by the Oak Ridge National Laboratory. It was positioned 1 meter from the scintillator and about 2 meters from the floor at the approximate center of a 4- by 10- by 12-meter room. The three organic liquid scintillators used were contained in glass cylinders with the following inside diameters and lengths (cm): 1.22 by 1.27, 2.16 by 2.41, and 4.65 by 5.15. The largest scintillator contained NE 213, and the other two contained NE 218 scintillator solutions.

The scintillators were mounted on RCA 8575 photomultiplier tubes. A modified Owens type pulse shape circuit as described in reference 5 was used. This circuit is used with a two-parameter pulse height analyzer to separate proton recoil and γ-ray events occurring in the scintillator. The proton recoil region of the two-parameter data set is summed by using the PREJUD computer code (ref. 6). Commercially available electronics were used. A circuit diagram of the spectrometer system used is shown in figure 1. The proton recoil spectra were measured from 200 keV to a little above 10 MeV proton energy by using four amplifier gain settings to provide adequate overlap and spectrum detail. Proton recoils due to room scattered neutrons were accounted for by using a water shadow cone.

All three scintillators were calibrated with a sodium-22 (Na^{22}) gamma ray source. The energy used for the half height of the Compton edge was 1.12 MeV. A calibration curve for the 1.22-centimeter-diameter scintillator is shown in figure 2. Also shown in the figure is a cobalt-60 (Co^{60}) distribution for this scintillator which shows that the two Co^{60} Compton edges are resolved. In figure 3 a low-energy calibration curve is shown for the 1.22-centimeter-diameter scintillator. The americium-241 (Am^{241}) source used has a γ-ray at low energy so that a photopeak is obtained by the organic scintillator. The resolution obtained from this photopeak at 0.060 MeV is 34 percent.

Since the spectrometer is calibrated with Compton recoil electrons provided by a convenient γ-ray source and then used to measure protons, the relation between the pulse heights of these two particles must be known. The relation used in the present work was measured by Verbinski, Burrus, Textor, Love, Zobel, and Hill (ref. 2); however, data were obtained in the present work at 2.8-MeV proton energy and the results are compared with the results of reference 2 in the section RESULTS AND DISCUSSION. These measurements were made by using the D(d, n) neutron reaction as a source of monoenergetic neutrons. The spectrometer was placed 1 meter from the target of a 150-kilovolt accelerator, and the proton recoil spectrum due to the 2.8-MeV neutrons was measured with the 1.22-centimeter-diameter by 1.27-centimeter-long scintillator. Background due to room scattered neutrons was accounted for by using a shadow cone. These data are shown in figure 4. The proton recoil distribution is roughly rectangular in shape as expected but rises with decreasing energy because of

the nonlinearity of proton pulse height as a function of energy. The shape would be rectangular for an ideal spectrometer.

DIFFERENTIAL SPECTRAL ANALYSIS

For an ideal scintillator that is thin enough so that multiple scattering is unimportant and yet thick enough so that wall effects are not important, the measured proton recoil distribution is a relatively simple function of the neutron spectrum and can be inverted to obtain the spectrum. Small corrections can then be applied to account for the deviation of the actual scintillator from an ideal one.

The differentiation method is based on neutron-proton isotropic scattering for which all proton recoil energies less than or equal to the incident neutron energy are equally probable. For monoenergetic neutrons the number of recoil protons per unit energy per second dN_p/dE_p is given by

$$\frac{dN_p}{dE_p} = A\epsilon \frac{\varphi}{E_n} \tag{1}$$

where φ is the number of neutrons per square centimeter per second at energy E_n (MeV) incident on a scintillator of area A (cm^2) normal to the beam, and ϵ is the incident neutron scattering probability of the hydrogen in the scintillator or efficiency of the scintillator. When polyenergetic neutrons are incident on the scintillator, the recoil-proton pulse height distribution dN_p/dE_p has contributions from all neutrons greater than or equal to E_p. Therefore,

$$\frac{dN_p}{dE_p} = A \int_{E_n=E_p}^{\infty} \epsilon(E_n) \frac{\varphi(E_n)}{E_n} dE_n \tag{2}$$

The neutron spectrum is obtained by differentiating equation (2) with respect to E_p and solving for $\varphi(E_n)$:

$$\varphi(E_n) = -\frac{E_n}{A\epsilon(E_n)} \left(\frac{d^2N_p}{dE_p^2} \right)_{E_n=E_p} \tag{3}$$

Since the scintillator light output does not vary linearly with recoil proton energy, the quantity measured is not dN_p/dE_p but dN_p/dE_B, where E_B is the energy of beta particles which are used to calibrate the spectrometer. Equation (3) must then be rewritten:

$$\varphi(E_n) = -\frac{E_n}{A\epsilon(E_n)}\left[\frac{d}{E_p}\left(\frac{dN_p}{dE_B}\frac{dE_B}{dE_p}\right)\right]_{E_p=E_n} \tag{4}$$

The variation of E_p with E_B used in this work was measured in reference 2. The measurements in reference 7 indicate that NE 213 and NE 218 are essentially the same with respect to the variation of E_p with E_B.

Multiple Scattering and Wall Effect Corrections

In a real scintillator there are multiple neutron scatterings, wall effects, and carbon interactions.

We have accounted for multiple scattering and wall effects by using the analysis of reference 8 in which two corrections are derived, L for proton leakage or wall effect and S for multiple scattering.

The leakage plus multiple scattering correction term is computed from the formula

$$L + S = \left[1 - 0.78\frac{R(E_n)}{\tau}\right] + 0.090\, N_h \tau \sigma(E_n) + 0.077\, N_h r \sigma(0.68\, E_n) \tag{5}$$

where $R(E_n)$ (mg/cm^2) is the range of a proton which receives the full neutron energy E_n (MeV), τ (mg/cm^2) is the scintillator thickness, N_h (atoms $\times 10^{24}$/cm^3) is the hydrogen atom density in the scintillator, $\sigma(E_n)$ (barns) is the neutron scattering cross section for hydrogen, and r (cm) is the radius of the scintillator. The first term of equation (5) accounts for the wall effect on the basis of 0.78 of that part of the scintillator volume in which protons can strike the wall. The correction is used as a flux divisor.

The calculated correction (L + S) is plotted in figure 5 for the 1.22- and 4.65-centimeter-diameter scintillators. For the small scintillator, the correction factor varies from 1.07 at 0.5 MeV to 0.91 at 10 MeV. The correction (0.07), therefore, is small enough to allow the method of differential spectral analysis to be applied without resulting in a significant error in the measured spectrum. For the large scintillator, multiple scattering dominates at all energies, and the correction factor is large, reaching 1.26 at 0.5 MeV. Unfortunately, the multiple scattering correction is probably the

least accurate of the two corrections because the nonlinearity of the proton light output causes these summed pulses from multiple scattering to appear significantly below the leading edge of the recoil distribution where the correction is applied. Therefore, the large scintillator requires calibrated monoenergetic neutron response functions to measure spectra accurately.

Carbon Interactions

Carbon interactions are the most difficult to account for in this type of analysis because of their effect on scintillator efficiency, as discussed in this section. However, pulses produced in the scintillator by carbon recoils and alpha particles from the C(n, α) reactions can be identified by pulse shape analysis and eliminated from the data. In the case of fission-like neutron spectra, the number of carbon reactions is small, and recoil pulses fall below most lower bias settings. Here the number of alpha particle pulses is small and can be ignored because of the high threshold for the C(n, α) reaction (6 MeV).

The characteristic shape of the proton recoil distribution can also be affected by neutrons interacting with carbon because a neutron can lose up to 28 percent of its energy in a carbon collision and then produce a recoil proton. The net effect of these processes and the hydrogen multiple scattering processes appears as an inflection in the proton recoil distribution at about 80 percent of the maximum energy. In the case of the data in figure 4, this inflection is not very evident within the statistics of the measurement, but it is very evident in the distributions shown in reference 2 for their larger scintillator. Since carbon multiple scattering processes, in which the collision involves only a small energy transfer, are indistinguishable from single hydrogen collision neutrons, they should be included in the scintillator efficiency. Proton recoils following large energy transfer carbon collisions cannot fall in the leading edge of the distribution and should not be included in the efficiency calculation.

Scintillator Efficiency Calculation

The efficiency of the scintillator ϵ is the probability that an incident neutron entering the detector will create a recoil proton. Since there is some self-shielding in all scintillators of practical size, the efficiency will vary depending on the angular distribution of the incident neutron flux.

Exact expressions for ϵ can be obtained for special cases. For the case of a parallel beam of neutrons incident on the flat face of a scintillator of thickness t and area A, the total number of first collisions that are scattering collisions with hydrogen is

$$A\epsilon = A\left(1 - e^{-\Sigma_t t}\right)\frac{\Sigma_H}{\Sigma_T} \tag{6}$$

where Σ_T is the total macroscopic cross section of the organic liquid and Σ_H is the hydrogen macroscopic cross section of the organic liquid. For the case of a parallel beam of neutrons incident on the curved surface of a cylindrical detector, a similar expression exists that involves an integral over the variable thickness.

However, neutron interactions with carbon alter the collision probability with hydrogen. The scintillator efficiency including carbon scattering contributions to the proton recoil distribution can be accurately computed from the following expression from reference 9:

$$A\epsilon = A\left(1 - e^{-\Sigma_{tr} t}\right)\frac{\Sigma_H}{\Sigma_H + \Sigma_{ctr}\rho_o} \tag{7}$$

where Σ_{tr} is the transport cross section, Σ_{ctr} is the carbon transport cross section, and ρ_o is the flat source escape probability (ref. 10). In expression (7), it is assumed that all carbon scattered sources are uniformly distributed. The expression was originally derived in reference 9 for sphere transmission analysis. In equation (7), hydrogen scattering by carbon atoms is treated as an absorption since further multiple scattering occurs within the time resolution of the spectrometer and simply increases the pulse size. An alternative to using equation (7) to calculate the total efficiency is

$$A\epsilon = A\left(1 - e^{-\Sigma_H t}\right) \tag{8}$$

which completely ignores the presence of carbon in the scintillator. This expression is indicated in reference 1 to give accurate results for scintillators up to 1 centimeter thick.

For the case of the scintillator immersed in an isotropic flux, the efficiency can be calculated by using methods developed for calculating resonance neutron capture in thermal reactors. Here the average fluxes in the two adjacent media are obtained by solving the coupled integral equations for the energy dependent fluxes that express the neutron balance in each region. The spatial transfer of neutrons between the adjacent media are obtained by means of their respective collision-escape probabilities ρ_o and application of a reciprocity condition. A large amount of experimental and analytical information is available on approximations to ρ_o and the accuracy of this method (ref. 10). The expression for the proton production rate per unit flux $A\epsilon$ is

$$A\epsilon = \rho_0 \Sigma_H At \tag{9}$$

for the first collision efficiency or

$$A\epsilon = \rho_0 \Sigma_T At \frac{\Sigma_H}{\Sigma_H + \rho_0 \Sigma_{ctr}} \tag{10}$$

for the total collision efficiency, where At is the volume of the scintillator.

Some insight into the applicability of various sized scintillators to differentiation analysis can be obtained from the previous expressions. Figures 6 and 7 show calculated efficiencies for various conditions as described in the figures.

In figure 6, the calculated efficiency times area is shown for a 4-65-centimeter-diameter by 5. 11-centimeter-long NE 213 scintillator. The upper curve is for the case of a parallel beam incident on the side of the scintillator and includes multiple scattering contributions. The three lower curves are for the types of flux incidence shown but do not include multiple scattering. Inclusion of multiple scattering increases the efficiency of this size scintillator approximately 15 percent at 1 MeV. As mentioned earlier, because proton recoils from carbon collisions cannot fall on the leading edge of the pulse height distribution, it is not clear that all of this calculated increased efficiency is applicable in differentiation analysis. Therefore, the true efficiency is bounded by the two upper curves. At higher energies this variation reduces to only about 5 percent. This energy dependent aspect of the calculated efficiency will give a small shape error to the derived spectrum. The calculated efficiencies in figure 6 also show a difference at 1 MeV of 18 percent for a parallel neutron beam incident on the flat surface compared to one incident on the curved surface of the scintillator, so that measurements with the larger scintillator are indicated to be sensitive to the angular distribution of the incident flux.

Similar efficiency calculations are shown in figure 7 for a 1. 22-centimeter-diameter by 1. 27-centimeter-long scintillator. The calculations show that multiple scattering is significant even for this small scintillator but that the efficiency variation involved is less than 5 percent at 1 MeV. The sensitivity of the efficiency of the smaller scintillator to the angular distribution of the incident neutron flux is also less than 5 percent for neutron energies greater than 1 MeV, which shows that flux measurements can be accurately made where the angular distribution is unknown. The efficiency is also low enough so that measurements can be made in a reactor.

Equations (4), (5), and (8) in the preceeding analysis are incorporated in the computer code TUNS written for the IBM 7094 computer. Parallel-beam neutrons incident on a curved surface can also be treated. A description of the code is given in appendix A, and the program listing is given in appendix B.

RESULTS AND DISCUSSION

Prior to comparing spectrum measurements of the PoBe source, it is of interest to analyze the proton recoil distribution for the 2.84-MeV monoenergetic neutron source presented in figure 4. Generally, the Compton electron energy corresponding to the half height of the leading edge of the proton recoil distribution is used as the beta energy corresponding to the neutron source energy; from the data in figure 4, this is 0.96 MeV. The calibration data for Ne-213 in reference 2 indicate that a 0.96-MeV beta corresponds to a proton energy of 2.78 MeV; this is 2 percent lower than the known neutron source energy of 2.84 MeV but within the 2 percent error quoted in reference 2.

There is some uncertainty in determination of the half height of the data in figure 4 since the full height is only characterized by a marked reduction in slope. An alternative method of determining the peak flux is to apply differentiation analysis to the data. The results show that the peak in the spectra can be fairly well determined but that very narrow slope-taking intervals must be used in the vicinity of the peak. It is therefore important that good counting statistics be obtained in order to use this method. The neutron spectra also show that between 2.0 and 2.4 MeV there is an indication of low residual flux values which may be attributed to multiple scattering in the scintillator.

The resolution of the spectrometer can be obtained from figure 8 and is 8.6 percent at the source energy of 2.84 MeV. The resolution at this energy of the 5-centimeter-diameter by 5-centimeter-long scintillator used at ORNL is given in reference 11 and is 20 percent. A second comparison can be made by using the data of figure 3, where the Am^{241} photopeak data which correspond to a neutron energy of 0.47 MeV show a resolution of 34 percent for the 1.22-centimeter-diameter scintillator. The resolution at this energy given in reference 12 for the 5- by 5-centimeter scintillator is 50 percent. The poor resolution reported shown in reference 12 is due in part to the inclusion of adequate smoothing in the FERDOR analysis of the measured data.

A significantly better resolution is indicated for the smaller scintillator. Although more data are desirable, the two-point comparison indicates a difference in shape of resolution as a function of energy for the two spectrometers.

The measured proton recoil spectra for the PoBe source using three scintillators are shown in figure 9. The small scale of the figure tends to smooth out much of the detail actually in the data, but some of the larger differences in the shapes of the three distributions are evident. Below a proton energy of 3 MeV (1 MeV beta) the curve for the 1.22-centimeter scintillator rises more rapidly than that of the larger scintillators because of less neutron self-shielding. At a proton energy of 10 MeV (5 MeV beta), a more pronounced inflection in the curve for the small scintillator is apparent because of its superior resolution.

Figures 10 to 12 show the results of the differentiation analysis for the PoBe source measurements. Figure 10 shows the spectrum obtained by using the NE 213 scintillator

that was 4.65 centimeters in diameter and 5.15 centimeters long. The data were analyzed by using the differentiation method and the unfolding method with the FERDOR code (ref. 13) and the data of reference 2. The FERDOR results were reduced 12 percent to correct for the greater length of our scintillator and to make our results directly compatible with the scintillator size used in reference 2. The spectrum obtained by differentiation is seen to be significantly lower than the spectrum generated by the FERDOR code, throughout the range of energy. The same proton recoil pulse height distribution data were used for both codes. The shapes of the two spectra are in general the same in both cases, except for a difference in energy location of the 3.4-MeV peak indicated by FERDOR and the presence of a peak at 2.2 MeV shown by the FERDOR results; a corresponding change in slope in the measured proton recoil distribution was not present at 2.2 MeV.

The deep valley that exists in the PoBe neutron spectra at approximately 1.5 MeV is a good test of proton recoil data differentiation analysis, since any deviation of the proton recoil distributions in the vicinity of 3.4 MeV from ideal shapes will be apparent in the unfolded spectra near 1.5 MeV. Thus, the change in slope of 3.4-MeV distributions at 80 percent of maximum pulse height due to carbon interactions, which are not accounted for by differentiation, could combine with small slope changes due to 2.2-MeV neutrons and result in a single slope change to produce the peak in the data at 3 MeV.

Figure 11 shows the spectrum obtained with the 2.16-centimeter-diameter scintillator. Also shown in the figure for comparison are the FERDOR results for the 4.65-centimeter-diameter scintillator. The uncertainty for the FERDOR results is not included for clarity. The differentiated results for this size scintillator show much better agreement with the FERDOR results than with the differentiated results for the 4.65-centimeter scintillator; however, there is still not a good match in the shape of the spectrum in the vicinity of 2 MeV.

Figure 12 shows the spectrum obtained with the 1.22-centimeter-diameter scintillator; this spectrum is also compared with the absolute FERDOR spectrum shown in figure 10. Comparison of the two spectra indicates good agreement with clear indications of the better resolution of the 1.22-centimeter-diameter scintillator. The small peak at 2 MeV indicated by FERDOR is also suggested in the data of figure 12. A second method of intercomparing the spectra is to compare the absolute integral flux. This has the advantage that the integral should be the same for two measured spectra even though the respective resolutions are different. Table I shows the integral flux above 0.5 MeV for the four determinations. These results show that the FERDOR integral flux is the same as that obtained for the two smaller scintillators but 15 percent higher than that obtained by differentiation for the 4.65-centimeter-diameter scintillator. The statistical uncertainty obtained with FERDOR is about one-half that obtained by differentiation. The statistical uncertainty is higher for the smallest scintillator because of insufficient counting times used in obtaining the proton recoil distribution.

The calculated total efficiency for proton production was used in the differentiation analysis. This efficiency includes protons produced following carbon collisions; therefore, it is not too surprising that the resulting flux for the 4.65-centimeter-diameter scintillator is lower than the small scintillator and FERDOR results. This comparison gives some credence to the postulate that only a small fraction of the protons produced following carbon collisions should be included in the scintillator efficiency used in the differentiation analysis, and that an effective efficiency for use in this analysis is the first collision efficiency. Unfortunately, part of the essentially constant percentage difference between the magnitude of the flux can also be explained by a large error in the L + S correction to the analysis, which also would result in low fluxes, as in the section Multiple Scattering and Wall Effect Corrections.

IMPLICATIONS OF RESULTS

Measurements have been made of the PoBe neutron spectrum by using three organic liquid scintillators of different sizes. Measurements were also made for 2.8-MeV neutrons from a D(dn) source by using a small 1.22-centimeter-diameter by 1.27-centimeter-long scintillator. An intercomparison of the absolute spectra was made from a calibrated unfolding analysis for the largest scintillator and a differentiation analysis for all the scintillators. Results indicated that spectra consistent in shape and magnitude can be obtained by differentiation for small liquid scintillators between 1 and 2 centimeters thick. If differentiation is used for scintillators as thick as 5 centimeters, significant shape differences in spectral valleys can result. The proper effective scintillator efficiency to be used in the analysis is indicated to be close to the first collision efficiency.

In the case of the smallest scintillator, the efficiency is shown to be insensitive to multiple scattering and the angular distribution of the incident flux. This characteristic and the inherently superior resolution of this size scintillator make its use desirable for flux measurements within diffusion media and in applications where high efficiency is not required. A computer code TUNS was written to analyze the data by differentiation analyses.

Lewis Research Center,
National Aeronautics and Space Administration,
Cleveland, Ohio, September 20, 1972,
503-10.

APPENDIX A

COMPUTER CODE TUNS

Code Description

The computer code TUNS which solves numerically equation (4) has been written in FORTRAN IV for the Lewis IBM 7094-II computer. The value of a derivative at a point is obtained as the average of the slopes from the point to its nearest neighbors, weighted inversely as the distance between points. Analytic expressions are used to compute $R(E_n)$, $\sigma(E_n)$, and $\sigma(0.68\ E_n)$ in equation (5) (ref. 14). The efficiency is calculated by using equation (8). A function subroutine SIMPS 1, (ref. 15) is used for integration in computing ϵ for a parallel beam of neutrons incident on the curved surface of the scintillator.

Input is described in the next section. The program output is in terms of neutron energy, flux, and the statistical error. Errors are computed from the standard deviations applied as input. The energy spacing between points is chosen to correspond to the spectrometer resolution. A wide spacing can be used and a small error will result, but spectral detail will be lost. The effect of the size of the interval from which the slope is determined on the accuracy of the spectra is discussed by Bennet (ref. 16).

Input Format for TUNS Code

Card number	Card column	Format	Variable name	Description
1-14	1-80	8G10.8	PE	dimensioned variable; should contain E_p in increasing order
15-28	1-80	8G10.8	DLDEP	dimensioned variable; should contain the values of dE_B/dE_p evaluated at E_p points for PE in increasing order of E_p
29-42	1-80	8G10.8	LT	dimensioned variable; should contain light output in terms of cobalts
43	2-73	12AG	TITLE	title card describing experiment
44	1-12	F12.5	DEBDL	conversion factor used in this report, 1.240 MeV/Co

Card number	Card column	Format	Variable name	Description
	13-24	F12.5	FACE	1.0 if flux is incident on flat surface
	28-30	I6	NPTS	number of input values (see card 4)
45	1-12	F12.5	NH	hydrogen atom density, atoms $\times 10^{24}/cm^3$
	13-24	F12.5	R	radius of scintillator, cm
	25-36	F12.5	H	height of scintillator, cm
	37-48	F12.5	BW	analyzed channel width, MeV
	49-60	F12.5	ADJ	analyzer live time, sec
	61-72	F12.5	WREF	1.0 if A, L, and S are desired as output
46(I)	26-28	I5	N(I)	card number
I = 1, . . ., NPTS	41-60	E20.9	DNDC(I)	counts per channel
	61-80	E20.9	ERR(I)	standard deviation in counts per channel

Card 46 (NPTS) may be followed by another set of data, beginning with a card 43; as many sets as desired may be run. Cards 46(1) to 46 (NPTS) may be obtained from code PREJUD (ref. 10).

APPENDIX B

PROGRAM LISTING

```
$TCP            TIME=1,PAGES=15,FORMS=PLAIN
$IBJOB          DEBUG
$IBFTC TUNSBC   DEBUG
      DIMENSION PE(109),EN(109),DLDEP(109),DLDE(109),DNDC(109),ARG(109),
     1DARG(107),FLUX(107),N(109),ERR(109),RELERR(109),FLUP(107),AER(109)
     2,FLO(107),SFLUX(109),DFLUX(109)
      REAL LT(109),LG(109),NH
      COMMON R,SIG
      EXTERNAL TRANS
      READ(5,1000) PE
      READ(5,1000) DLDEP
      READ(5,1000) LT
    1 READ(5,2500)
      WRITE(6,2400)
      WRITE(6,2500)
      READ(5,1150) DEBDL, FACE, NPTS
      READ(5,1100)NH,R,H,BW,ADJ,WREF
      READ(5,1200) (N(I),DNDC(I),ERR(I),I=1,NPTS)
      WRITE(6,1050) DEBDL,NH,R,H,BW,ADJ
      WRITE(6,1060) NPTS
      IF(FACE-1.0) 3,4,3
    3 WRITE(6,1075)
      REF=SQRT(2.0*R*H/3.1416)
      GO TO 5
    4 WRITE(6,1080)
      REF=R
    5 WRITE(6,1085)
      WRITE(6,1090) (I,N(I),DNDC(I),ERR(I), I=1,NPTS)
      DO 10 I=1,NPTS
      IF(N(I).EQ.28.OR.N(I).EQ.30.OR.N(I).EQ.32.OR.N(I).EQ.34) GO TO 6
      GO TO 7
    6 WRITE(6,1070) N(I)
      STOP
    7 IF(N(I).EQ.29) N(I)=28
      IF(N(I).EQ.31) N(I)=29
      IF(N(I).EQ.33) N(I)=30
      IF(N(I).GT.34) N(I)=N(I)-4
      IF(N(I).GT.109) GO TO 8
      GO TO 9
    8 WRITE(6,1065)
      STOP
    9 M=N(I)
      EN(I)=PE(M)
      DLDE(I)=DLDEP(M)
      LG(I)=LT(M)
   10 CONTINUE
   12 DO 14 I=1,NPTS
      DNDL=DEBDL*DNDC(I)/BW
      ARG(I)=DNDL*DLDE(I)
      AER(I)=DLDE(I)*DEBDL*ERR(I)/BW
   14 CONTINUE
      MPTS=NPTS-2
```

```
15 DO 20 I=1,MPTS
   DA=(ARG(I+1)-ARG(I))/(LG(I+1)-LG(I))
   DB=(ARG(I+2)-ARG(I+1))/(LG(I+2)-LG(I+1))
   DWA=(LG(I+2)-LG(I+1))*DA
   DWB=(LG(I+1)-LG(I))*DB
   DARG(I)=(DWA+DWB)/(LG(I+2)-LG(I))
   RELERR(I)=ABS(SQRT(AER(I)**2+AER(I+2)**2)/(ARG(I)-ARG(I+2)))
20 CONTINUE
   IF(WREF-1.0) 25,24,25
24 WRITE(6,1600)
25 DO 50 I=1,MPTS
   BOT=1.0+7.417*EN(I+1)+0.1105*EN(I+1)**2
   FIRST=17.6024/BOT
   BOTT=1.0+0.2427*EN(I+1)+0.0028*EN(I+1)**2
   SEC=2.7181/BOTT
   SIGH=FIRST+SEC
   SIG=NH*SIGH
   K=0
   IF(FACE-1.0) 27,29,27
27 SIM=SIMPS1(0.0,R,TRANS,K)
   EF=R-SIM
   A=2.0*R*H
   EFF=EF/R*A
   SIMR=SIM/R
   TH=ALOG(SIMR)
   THEF=-1.0*TH/SIG
   GO TO 31
29 EF=1.0-EXP(-1.0*SIG*H)
   A=3.1416*R*R
   EFF=EF*A
   THEF=H
31 ENL=0.068*EN(I+1)
   DOWN=1.0+7.417*ENL+0.1105*ENL**2
   ONE=17.6024/DOWN
   DOWNN=1.0+0.2427*ENL+0.0028*ENL**2
   TWO=2.7181/DOWNN
   SIGHL=ONE+TWO
   RM=1.7382*(EN(I+1)+0.15045)**1.8194
   RANGE=RM/870.
   ESC=1.0-0.780*RANGE/THEF
   SESA=0.090*NH*THEF*SIGH
   SESB=0.077*NH*REF*SIGHL
   SESC=SESA+SESB
   BEE=ESC+SESC
   IF(WREF-1.0) 36,34,36
34 WRITE(6,1700) EN(I+1),EFF,K,ESC,SESC,RANGE
36 ONDE=-1.0*EN(I+1)*OLDE(I+1)*DARG(I)/EFF/BEE
   FLUX(I)=ONDE/ADJ
   PREC=RELERR(I)*FLUX(I)
   FLUP(I)=FLUX(I)+PREC
   FLO(I)=FLUX(I)-PREC
50 CONTINUE
   IM = 0
   SFLUX(1) = 0.
   UFLUX(108) = 0.
   DO 70 I = 2,MPTS
   J = MPTS + 2 - I
   SFLUX(I) = SFLUX(I-1) + FLUX(I) * (EN(I+1) - EN(I))
   UFLUX(J) = UFLUX(J+1) + FLUX(J) * (EN(J+1) - EN(J))
```

```
      IF (FLUX(I) .GE. 0.) GO TO 70
      IM = I
      SFLUX(I) = 0.
   70 CONTINUE
      IF (IM .EQ. 0) GO TO 100
      DO 80 I = 1,IM
      SFLUX(I) = 0.
   80 UFLUX(I) = UFLUX(IM+1)
      IM = IM + 1
      SFLUX(IM) = FLUX(IM) * (EN(IM+1) - EN(IM))
  100 WRITE(6,1500)
      WRITE(6,2000) (I,N(I+1),EN(I+1),FLUX(I),FLUP(I),FLO(I),SFLUX(I),
     *UFLUX(I),I = 1,MPTS)
      GO TO 1
 1000 FORMAT (8G10.8)
 1050 FORMAT(1H0,66HFACTOR FOR CONVERTING COUNTS PER MEV BETA TO COUNTS
     1PER COBALT IS ,1PE12.5//30H THE HYDROGEN ATOM DENSITY IS ,1PE12.5/
     2/35H THE RADIUS OF THE SCINTILLATOR IS ,1PE12.5//35H THE HEIGHT OF
     3 THE SCINTILLATOR IS ,1PE12.5//28H THE BIN WIDTH (M VALUE) IS ,1PE
     412.5//31H THE FLUX ADJUSTMENT FACTOR IS ,1PE12.5)
 1060 FORMAT(1H0,30HTHE NUMBER OF INPUT VALUES IS ,I3)
 1065 FORMAT(1H0,35HERROR- LOC. NO. IS GREATER THAN 109)
 1070 FORMAT(1H0,52HERROR- CARD SHOULD BE REMOVED FROM DATA. CARD NO. =
     1,I3)
 1075 FORMAT(1H0,62HTHE FLUX IS INCIDENT ON THE CURVED SURFACE OF THE SC
     1INTILLATOR)
 1080 FORMAT(1H0,60HTHE FLUX IS INCIDENT ON THE FLAT SURFACE OF THE SCIN
     1TILLATOR)
 1085 FORMAT(1H0,6X,9HINPUT NO.,10X,8HCARD NO.,20X,6HCOUNTS,14X,9HSTD. D
     1EV.)
 1090 FORMAT(6X,I3,18X,I3,20X,1PE12.5,8X,1PE12.5)
 1100 FORMAT (6F12.5)
 1150 FORMAT(2F12.5,I6)
 1200 FORMAT(23X,I5,12X,2E20.9)
 1500 FORMAT (1HL,80X,2(10HINTEGRATED,4X)/4X,7HPT. NO.,2X,8HLOC. NO.,8X,
     16HENERGY,10X,4HFLUX,3X,11HUPPER BOUND,3X,11HLOWER BOUND,2X,12HFLUX
     2 BELOW E,2X,12HFLUX ABOVE E//)
 1600 FORMAT(1H0,6X,6HENERGY,13X,10HEFFICIENCY,6X,4HERRP,21X,7HLEAKAGE,
     112X,7HSECSCAT,12X,5HRANGE)
 1700 FORMAT(2(4X,1PE12.5,4X),I5,15X,3(4X,1PE12.5,4X))
 2000 FORMAT(8X,I3,I10,1P6E14.5)
 2400 FORMAT(1H1)
 2500 FORMAT(80H
     1
      END
$IBFTC TRANSM
      FUNCTION TRANS(X)
      COMMON R,SIG
      PL=-2.0*SIG*SQRT(R**2-X**2)
      TRANS=EXP(PL)
      RETURN
      END
```

REFERENCES

1. Swartz, C. D.; and Owen, George E.: Recoil Detection in Scintillators. Fast Neutron Physics. Part I: Techniques. J. B. Marion, and J. L. Fowler, eds., Interscience Publishers, Inc., 1960, pp. 211-246.

2. Verbinski, V. V.; Burrus, W. R.; Love, T. A.; Zobel, W.; Hill, N. W.; and Textor, R.: Calibration of an Organic Scintillator For Neutron Spectroscopy. Nucl. Inst. Methods, vol. 65, 1968, pp. 8-25.

3. Straker, E. A.; Burgart, C. E.; Love, T. A.; and Freestone, R. M., Jr.: Simultaneous Determination of Fast-Neutron Spectra by Time-of-Flight and Pulse Height Unfolding Techniques. Rep. ORNL-TM-3371, Oak Ridge National Lab. (AD-723181), Apr. 5, 1971.

4. Shook, Donald F.: A Small Differentiable Liquid Scintillator Neutron Spectrometer. Trans. Am. Nucl. Soc., vol. 13, no. 1, June 1970, pp. 430-431.

5. Shook, Donald F.; and Blue, James W.: Circuit Modification Aids in Atomic Particle Discrimination. NASA Tech. Brief 70-10689, 1970.

6. Semler, Thor T.: PREJUD-A Computer Code for the Preliminary Analysis of Two-Dimensional Pulse Height Analyzer Data. NASA TM X-2181, 1971.

7. Pohl, B. A.; Anderson, J. D.; McClure, J. W.; and Wong, C.: Method for Determining Scintillator Response Functions for Fast Neutrons. Rep. UCRL-50653, California Univ., Lawrence Radiation Lab., Apr. 29, 1969.

8. Broek, H. W.; and Anderson, C. E.: The Stilbene Scintillation Crystal as a Spectrometer for Continuous Fast-Neutron Spectra. Rev. Sci. Inst., vol. 31, no. 10, Oct. 1960, pp. 1063-1069.

9. Bethe, H. A.; Beyster, J. R.; and Carter, R. E.: Inelastic Cross-Sections for Fission-Spectrum Neutrons - I. J. Nucl. Energy, vol. 3, no. 3, 1956, pp. 207-223.

10. Case, K. M.; deHoffman, F.; and Placzek, R.: Introduction to the Theory of Neutron Diffusion. Los Alamos Scientific Laboratories, 1953.

11. Dresner, Lawrence: Resonance Absorption in Nuclear Reactors. Pergamon Press, 1960.

12. Straker, E. A.: Experimental Evaluation of Minima in the Total Neutron Cross Sections of Several Shielding Materials. Nucl. Sci. Eng., vol. 34, no. 2, Nov. 1968, pp. 114-121.

13. Burrus, W. R.: Utilization of a Priori Information by Means of Mathematical Programming in the Statistical Interpretation of Measured Distributions. Rep. ORNL-3743, Oak Ridge National Lab. (NASA CR-63442), June 1965.

14. Toms, M. Elaine: Stilbene and NE 213 Characteristics Related to Their Use for Neutron Spectroscopy. IEEE Trans. on Nucl. Sci., vol. NS-17, no. 3, June 1970, pp. 107-114.

15. Canright, R. Bruce, Jr.; and Semler, Thor T.: Comparison of Numerical Techniques for the Evaluation of the Doppler Broadening Functions $\psi(x, \theta)$ and (x, θ). NASA TM X-2559, 1972.

16. Bennett, E. F.: Fast Neutron Spectroscopy by Proton-Recoil Proportional Counting. Nucl. Sci. Eng., vol. 27, no. 1, Jan. 1967, pp. 16-27.

TABLE I. - MEASURED TOTAL FLUX ABOVE 0.5 MeV AT 1 METER FROM POLONIUM-BERYLLIUM SOURCE

Scintillator size, cm	Unfolding method	Total flux, neutrons/(cm^2)(sec)
4.65 by 5.15	FERDOR Differentiation	99.0±0.8 85.8±1.7
2.16 by 2.41	Differentiation	99.1±1.9
1.22 by 1.27	Differentiation	103±2.8

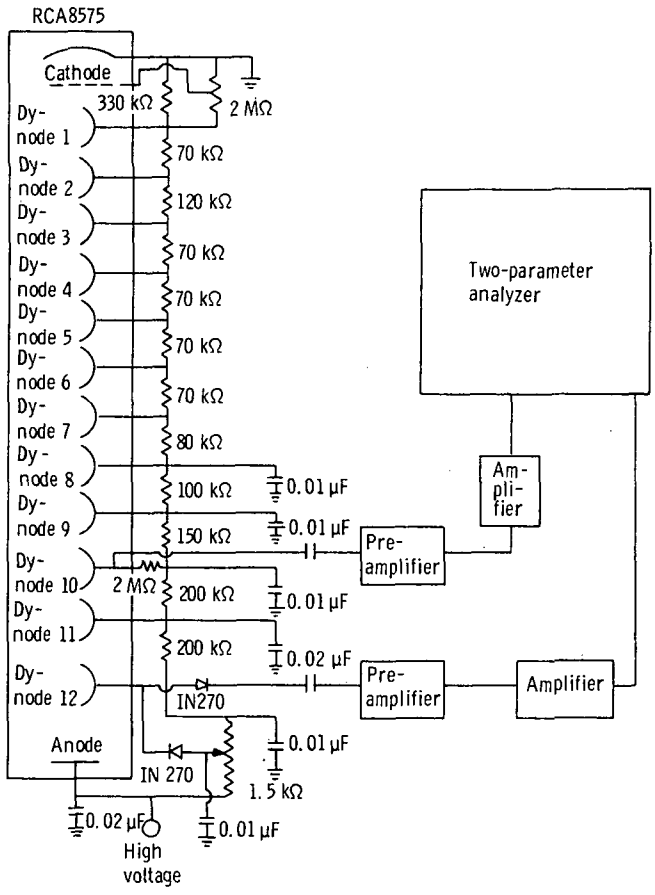

Figure 1. - Spectrometer block diagram and photomultiplier tube base circuit.

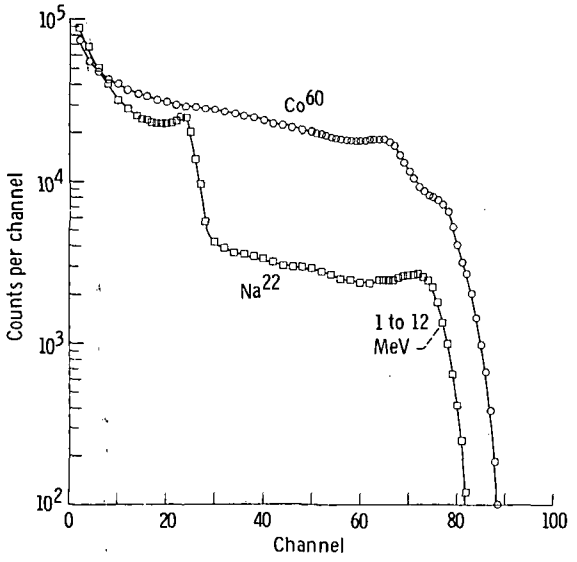

Figure 2. - Cobalt-60 and sodium-22 calibration curves for 1.22-centimeter-diameter scintillator.

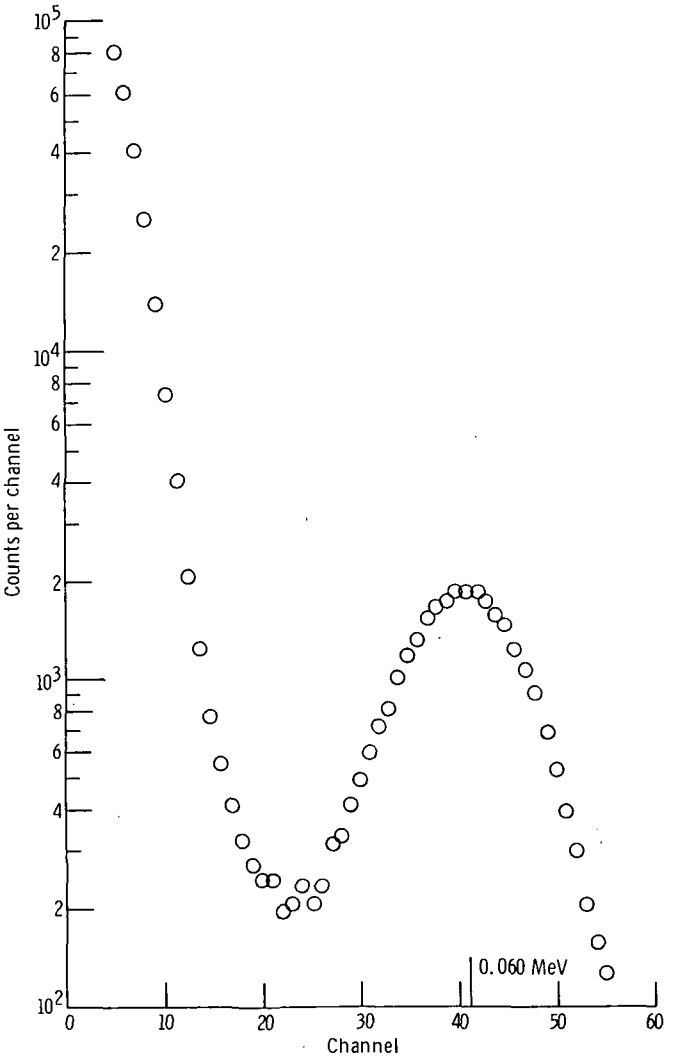

Figure 3. - Americium-241 calibration curve for 1.22-centimeter-diameter scintillator.

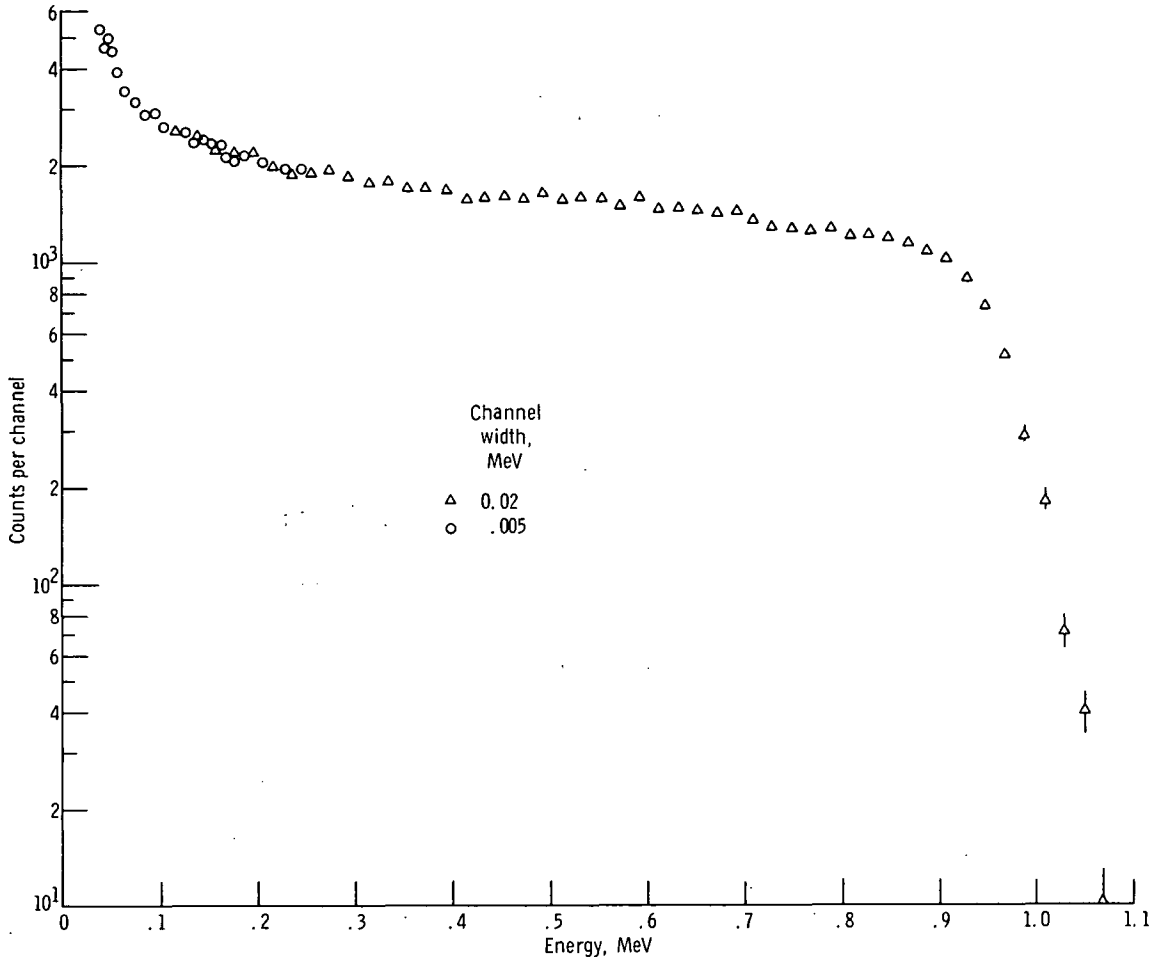

Figure 4. - Proton recoil distribution from 2.8-MeV neutrons using 1.22-centimeter-diameter scintillator.

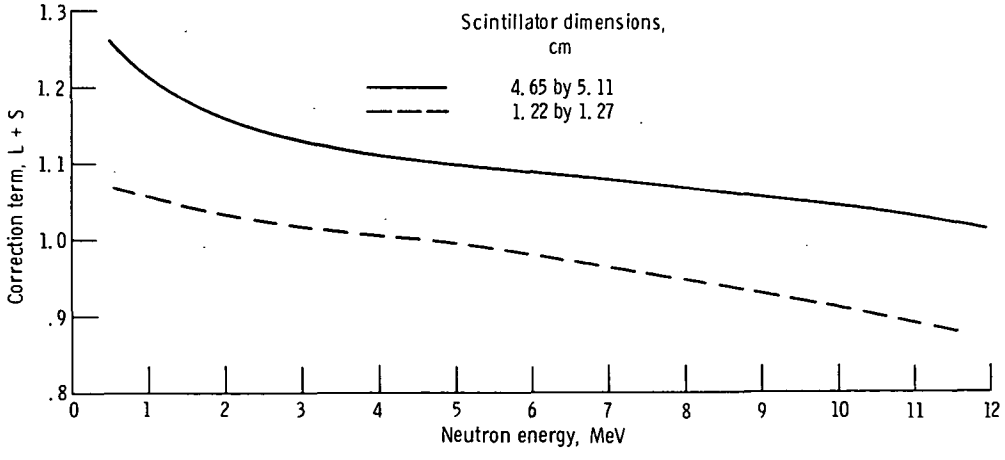

Figure 5. - Wall effect plus multiple scattering correction (L + S).

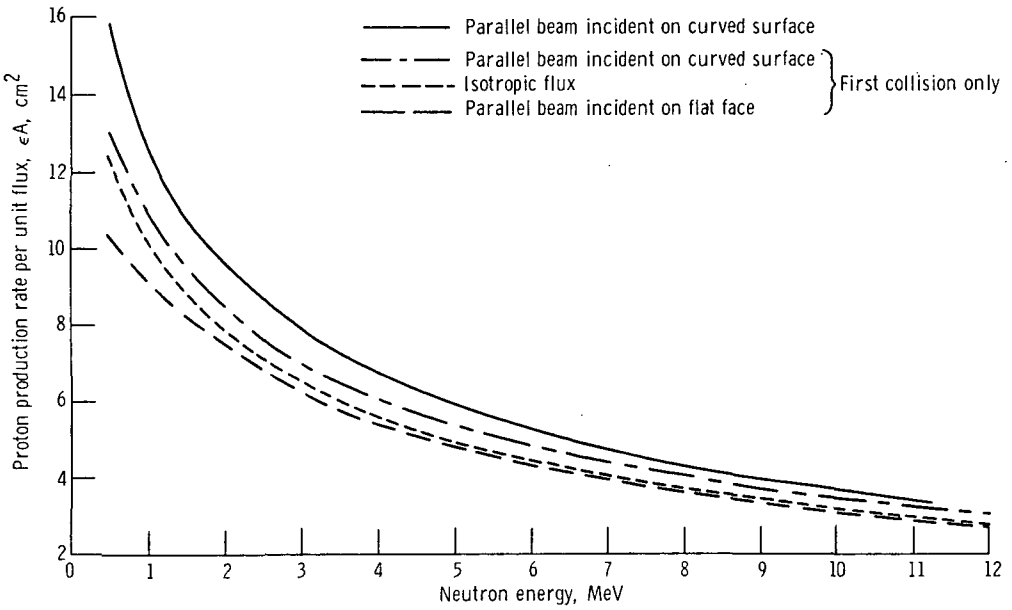

Figure 6. - Proton production rate per unit flux for 4.65-centimeter-diameter by 5.11-centimeter-long scintillator.

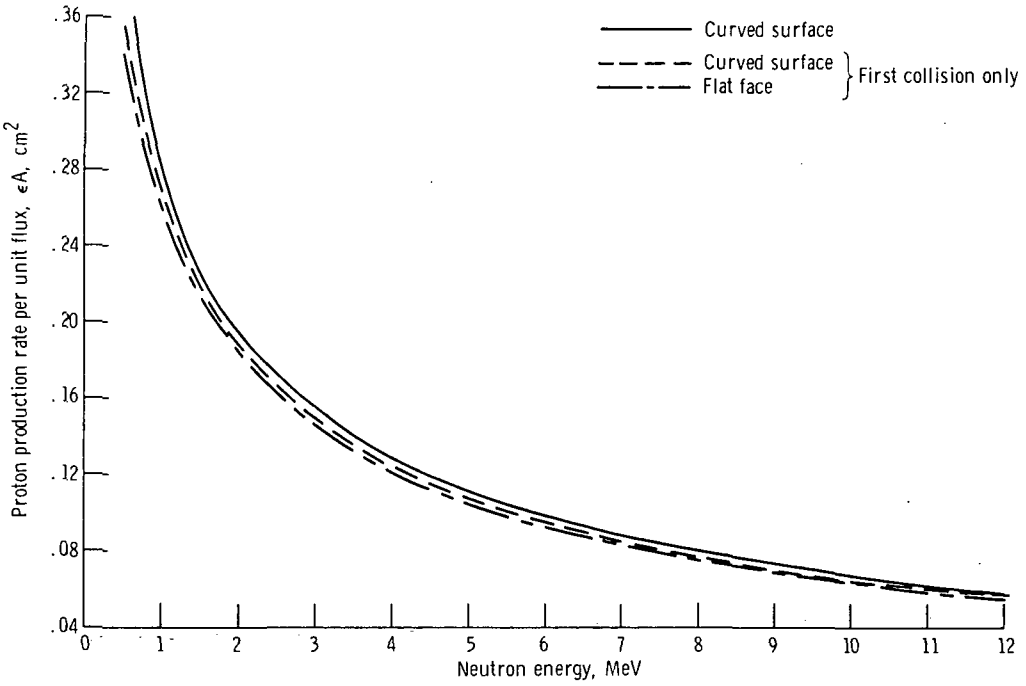

Figure 7. - Proton production rate per unit flux for 1.22-centimeter-diameter by 1.27-centimeter-long scintillator. Parallel beam incident on curved and flat surfaces.

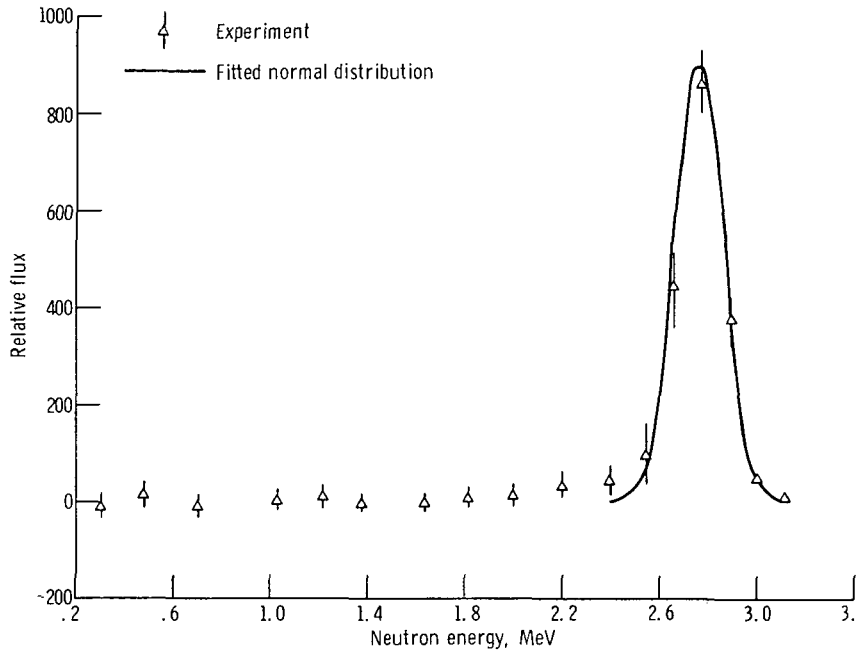

Figure 8. - Neutron source spectra from D(dn) reaction at 0^{o} from target. Deuteron energy, 100 kilovolts; measured with 1.22-centimeter-diameter by 1.27-centimeter-long scintillator.

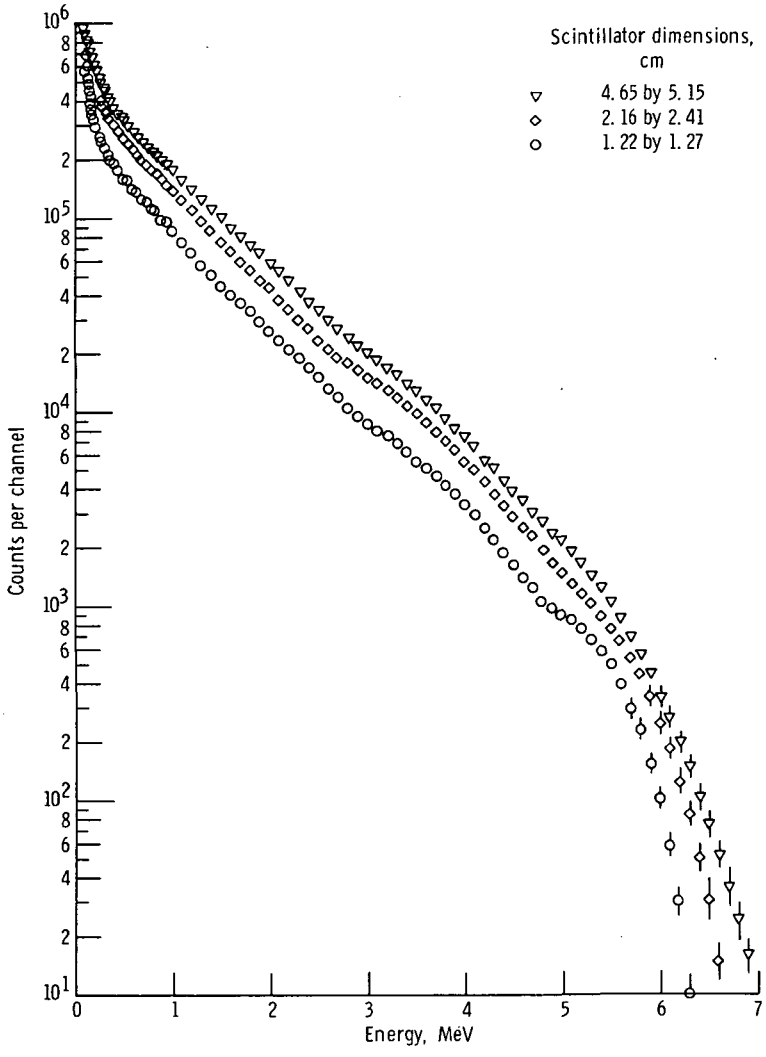

Figure 9. - Proton recoil distribution for three scintillator sizes.

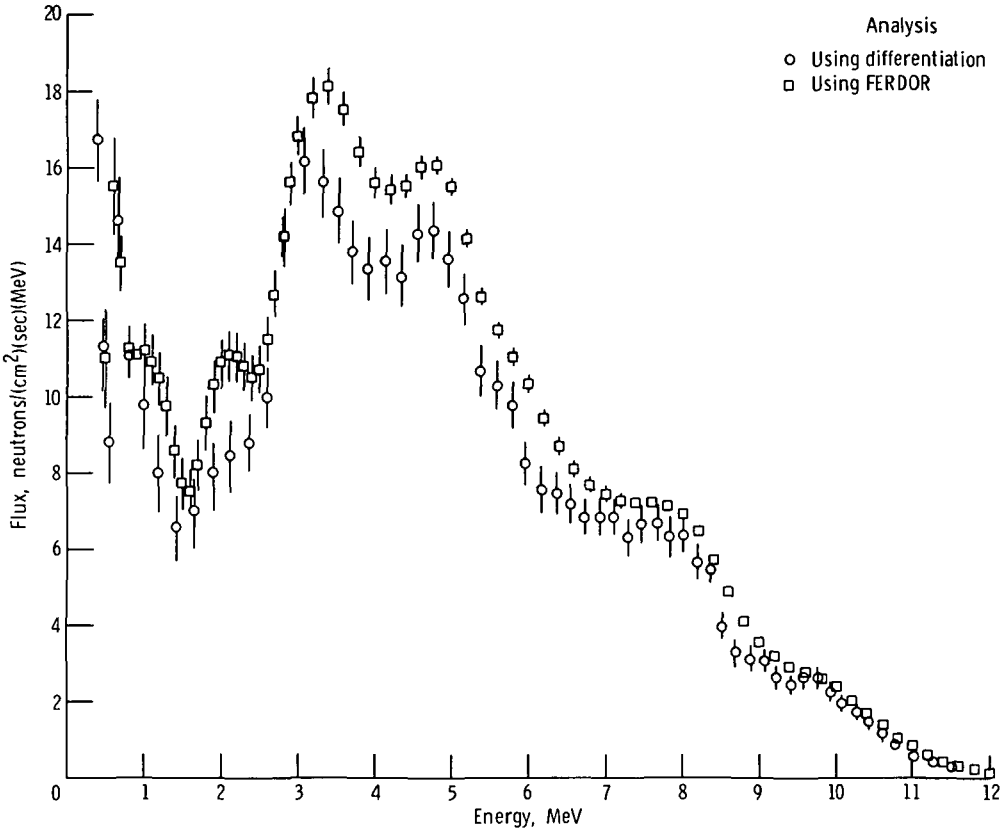

Figure 10. - Polonium-beryllium source measured with 4.65-centimeter-diameter by 5.15-centimeter-long scintillator.

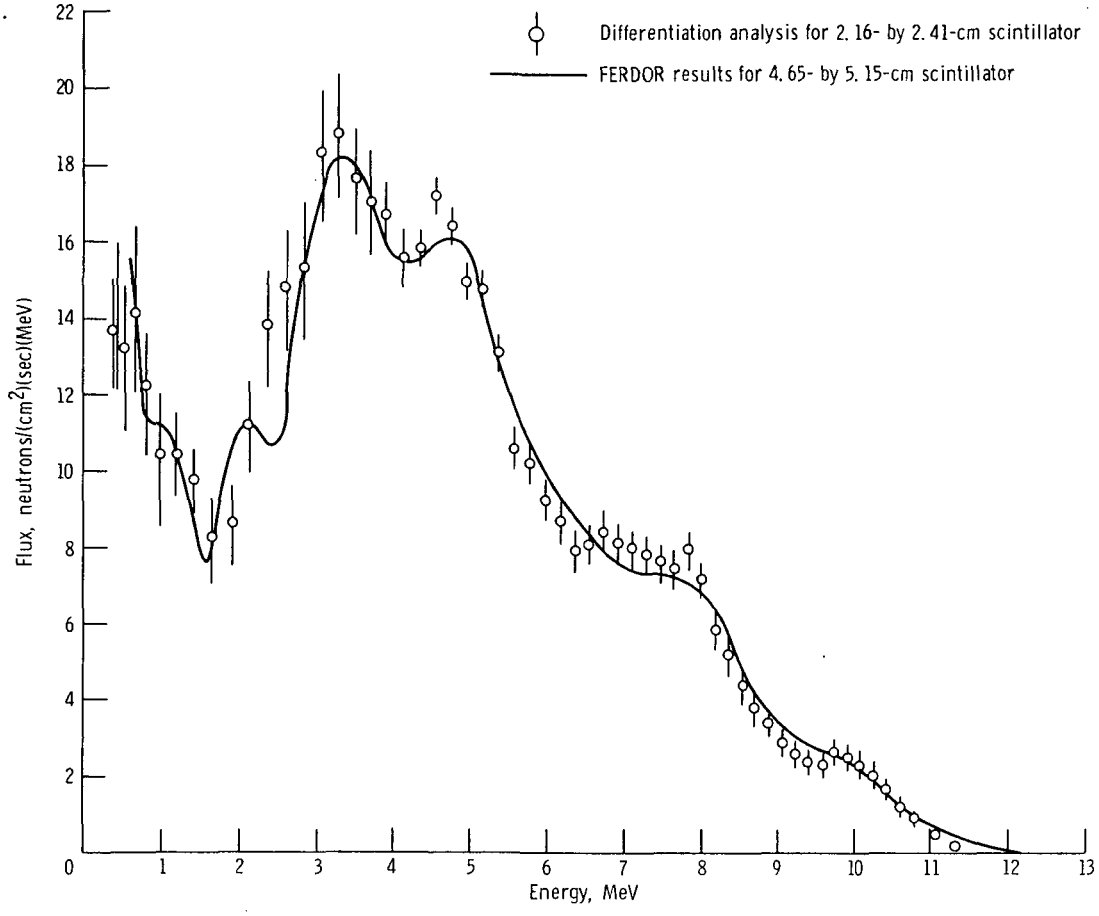

Figure 11. - Comparison of differentiation analysis and FERDOR results for polonium-beryllium neutron spectrum.

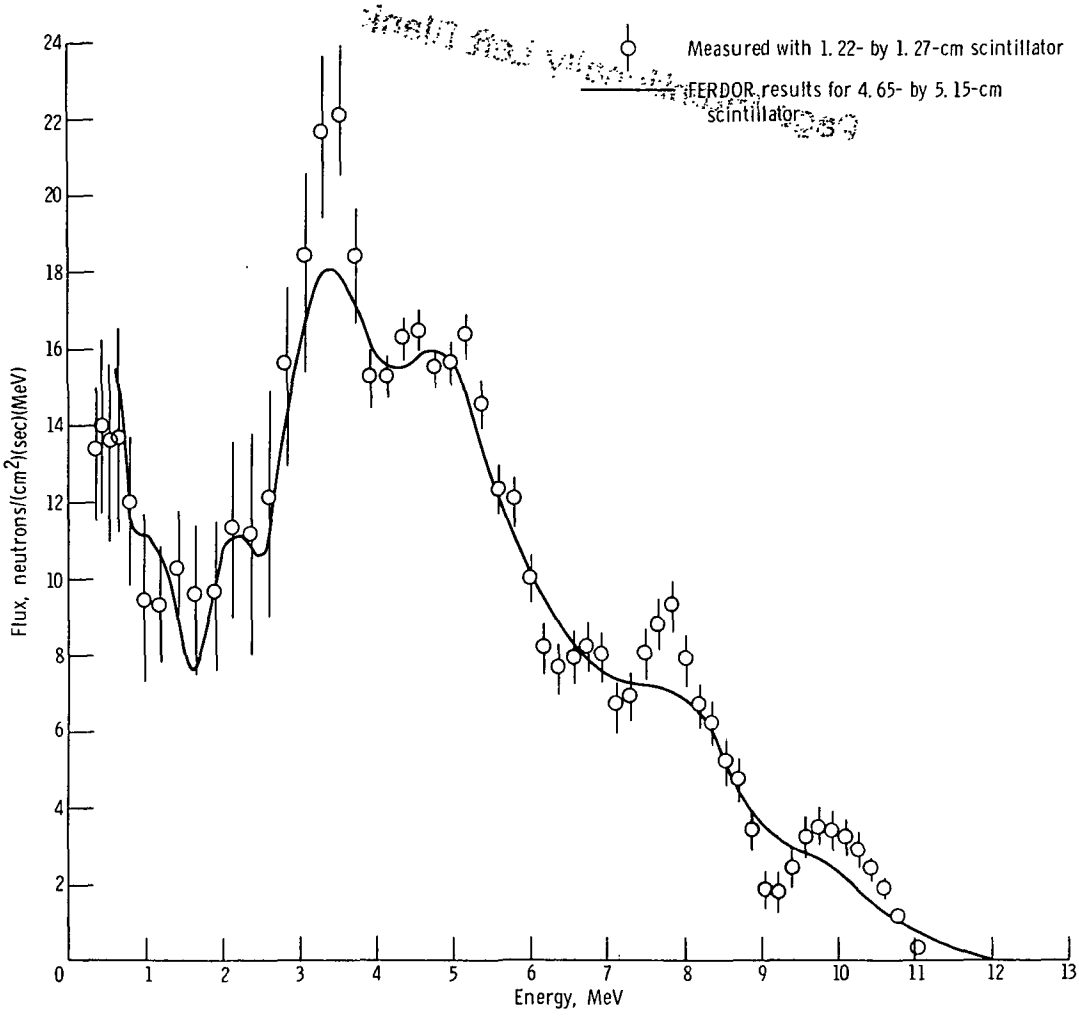

Figure 12. - Comparison of measured and FERDOR results for polonium-beryllium neutron spectrum.

NATIONAL AERONAUTICS AND SPACE ADMINISTRATION
WASHINGTON, D.C. 20546

OFFICIAL BUSINESS
PENALTY FOR PRIVATE USE $300

SPECIAL FOURTH-CLASS RATE BOOK

POSTAGE AND FEES PAID
NATIONAL AERONAUTICS AND SPACE ADMINISTRATION
451

U.S. MAIL

POSTMASTER: If Undeliverable (Section 158 Postal Manual) Do Not Return

"The aeronautical and space activities of the United States shall be conducted so as to contribute . . . to the expansion of human knowledge of phenomena in the atmosphere and space. The Administration shall provide for the widest practicable and appropriate dissemination of information concerning its activities and the results thereof."

—NATIONAL AERONAUTICS AND SPACE ACT OF 1958

NASA SCIENTIFIC AND TECHNICAL PUBLICATIONS

TECHNICAL REPORTS: Scientific and technical information considered important, complete, and a lasting contribution to existing knowledge.

TECHNICAL NOTES: Information less broad in scope but nevertheless of importance as a contribution to existing knowledge.

TECHNICAL MEMORANDUMS: Information receiving limited distribution because of preliminary data, security classification, or other reasons. Also includes conference proceedings with either limited or unlimited distribution.

CONTRACTOR REPORTS: Scientific and technical information generated under a NASA contract or grant and considered an important contribution to existing knowledge.

TECHNICAL TRANSLATIONS: Information published in a foreign language considered to merit NASA distribution in English.

SPECIAL PUBLICATIONS: Information derived from or of value to NASA activities. Publications include final reports of major projects, monographs, data compilations, handbooks, sourcebooks, and special bibliographies.

TECHNOLOGY UTILIZATION PUBLICATIONS: Information on technology used by NASA that may be of particular interest in commercial and other non-aerospace applications. Publications include Tech Briefs, Technology Utilization Reports and Technology Surveys.

Details on the availability of these publications may be obtained from:

SCIENTIFIC AND TECHNICAL INFORMATION OFFICE

NATIONAL AERONAUTICS AND SPACE ADMINISTRATION

Washington, D.C. 20546